AIP | Applied Physics Letters

Electrochemical nanopatterning of Ag on solid-state ionic conductor RbAg4I5 using atomic force microscopy

Minhwan Lee, Ryan O'Hayre, Fritz B. Prinz, and Turgut M. Gür

Citation: Appl. Phys. Lett. **85**, 3552 (2004); doi: 10.1063/1.1807964
View online: http://dx.doi.org/10.1063/1.1807964
View Table of Contents: http://apl.aip.org/resource/1/APPLAB/v85/i16
Published by the American Institute of Physics.

Electrochemical nanopatterning of Ag on solid-state ionic conductor $RbAg_4I_5$ using atomic force microscopy

Minhwan Lee,[a] Ryan O'Hayre, and Fritz B. Prinz
Rapid Prototyping Laboratory, Stanford University, Stanford, California 94305-303

Turgut M. Gür
H2onsite, Inc., Millbrae, California 94030

(Received 1 June 2004; accepted 20 August 2004)

This report introduces an electrochemical nanopatterning technique performed under ambient conditions without involving a liquid vessel or probe-to-sample material transfer. Patterning is accomplished by solid-state electrochemical nanodeposition of Ag clusters on the surface of the solid ionic conductor $RbAg_4I_5$ using an atomic force microscopy probe. Application of negative voltage pulses on the probe relative to an Ag film counter electrode on an $RbAg_4I_5$ sample induces nanometer-sized Ag deposition on the ion conductor around the probe. The patterned Ag particles are 0.5–70 nm high and 20–700 nm in diameter. The effect of the amplitude and duration of bias voltage on the size and shape of deposited Ag clusters is also shown. © *2004 American Institute of Physics*. [DOI: 10.1063/1.1807964]

In the past decade, nanolithography techniques using scanning probe microscopy have been widely investigated. A variety of patterning techniques have been introduced, based on phenomena that include pure mechanical effects,[1–3] thermomechanical effects,[4,5] exposure of resist to electronic current,[6–9] electrochemical reactions in solutions,[10–13] local oxidation of Si,[14–17] direct delivery of molecules,[18,19] and electrostatic polymer modification.[20,21] In this letter, we report a nanolithography technique that generates topological patterns by electrochemical reduction of metal on a solid-state ion conducting membrane.

To demonstrate this concept, we have selected $RbAg_4I_5$, which is known to be a fast and selective Ag ion conducting electrolyte that exhibits the highest known room temperature ionic conductivity of 0.27 S/cm.[22] By applying a voltage bias for a short time period between two electrodes—one is a Ag coated AFM tip and the other is a sputtered Ag film bulk counter electrode attached to the $RbAg_4I_5$ ion conductor—we could draw Ag atoms from the counter electrode to the tip and eventually deposit on the ion conductor in the vicinity of the probe. When negative bias is applied to the tip, silver atoms at the counter electrode are oxidized into positively charged ions, which then migrate through the ion conductor to the tip electrode due to the applied electric field. The silver ions are electrochemically reduced into Ag atoms at the tip, resulting in nano-size Ag patterns. Alternatively, local reduction to metallic Ag may also occur even without bulk mass transport from the counter electrode, because Ag^+ ions are abundant in the film and the tip electrode is small compared to the sample. This belief is supported by the exponential current–voltage response of the system (discussed later in this letter). In fact, electrochemical nanopatterning of Ag is observed to occur even without a counter Ag electrode. In such circumstances, the nanopatterning technique likely causes slight changes to the stoichiometery of the surrounding $RbAg_4I_5$ material as local Ag^+ ions are reduced to Ag metal.

[a]Author to whom correspondence should be addressed; electronic mail: piecoco@stanford.edu

While we illustrate the technique on $RbAg_4I_5$, it should also be applicable to a number of other solid ion conductor systems. Compared to some of the previous nanolithography processes listed earlier, this technique exhibits operational simplicity, since localized patterning is directed only by the application of electrical bias pulses through a probe tip. Additionally, this process is achieved under atmospheric pressure without any apparatus for special environment.

To make $RbAg_4I_5$ samples, a stoichiometric (83 mol% AgI) mixture of RbI and AgI powder (Alfa Aesar) was placed in a ceramic crucible. The mixture was heated to 450 °C at a rate of 10 °C/min in a glass-tube furnace. After treatment at 450 °C for 1h, the mixture was cooled down slowly. The resulting sample was crushed into powder and verified to be $RbAg_4I_5$ by x-ray diffraction analysis. This powder was stored in an opaque chamber with desiccant under vacuum when not used because $RbAg_4I_5$ is light and humidity sensitive.[23] To fabricate $RbAg_4I_5$ samples for the electrochemical nanopatterning experiments, a few grams of $RbAg_4I_5$ powder were evenly placed on a bare Si wafer and heated again to 450 °C at a rate of 10 °C/min. After heating at 450 °C for 10 min, the mixture was slowly cooled, resulting in a 0.2- to 0.7-mm-thick $RbAg_4I_5$ film on Si wafer. To form the bulk Ag counter electrode, an Ag film was partially sputtered on the $RbAg_4I_5$ sample. The working electrode, which directs the localized nanopatterning, is a conductive AFM probe.

Figure 1 shows a simple schematic for our nanopatterning experiment. A commercial AFM system is used for this work (PicoScan II, Molecular Imaging©). Since probes with high force constant incurred topological change by mechanical scratching during scanning, soft probes (0.1–0.3 N/m, MikroMasch©) were mostly used. Sample-to-tip bias was applied by utilizing the current sensing module (CSAFM) embedded in the PicoScan II AFM system through which voltage pulse up to ±10 V for an arbitrary period of time between 1 and 65 535 μs could be provided.

Electrochemical deposition of Ag was achieved by applying voltage pulses between an AFM probe and an Ag film counter electrode located on the back side of the $RbAg_4I_5$

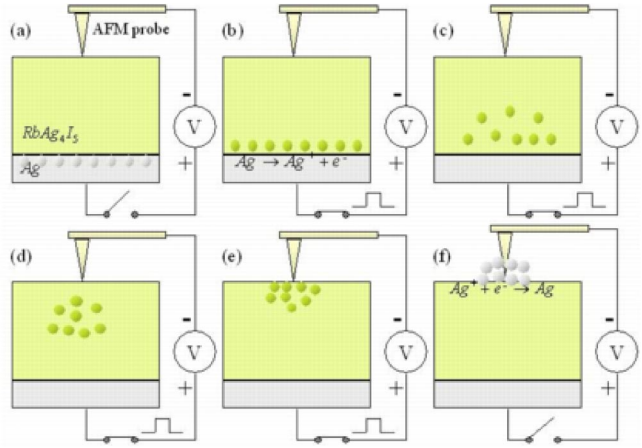

FIG. 1. Simplified schematic diagram of the experimental setup for nano-patterning of Ag on $RbAg_4I_5$, showing the time evolution of Ag atoms and ions under the voltage bias. Oxidation and reduction processes are depicted in steps (b) and (f), respectively. The migration of silver ions in the ion conductor under the electric field is shown in steps between (b) and (e). Drawing not to scale.

film, following Fig. 1. Before deposition, the open circuit voltage (OCV) of the Ag-tip/$RbAg_4I_5$/Ag-film system was sought for using the $I-V$ spectroscopy capability of our AFM system.[24] Even though this voltage should be zero ideally—since the chemical nature and environment of the two electrodes should be the same—in reality, the OCV value varies within ± a few tens of millivolts. A typical $I-V$ curve for the system is shown in Fig. 2. This $I-V$ curve was obtained by sweeping the potential of the Ag film from +100 to −100 mV versus the AFM probe at the rate of −100 mV/s.

Prior to patterning, the sample topology was scanned several times, during which a zero-current potential was held between the two electrodes in order to avoid unintentional bias-induced topological change. After the topological image was stabilized, the tip was moved to a specific position where Ag deposition was desired. To induce Ag deposition by electrochemical reduction at the tip, negative tip-to-sample bias pulses of 50 mV–2 V lasting from 0.5 to 50 ms were used. After pulse application, the topology was scanned again to investigate the size and shape of Ag deposition.

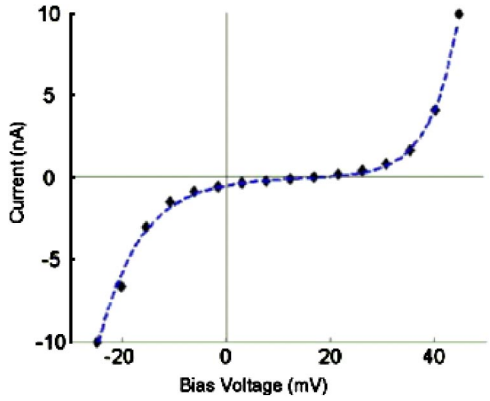

FIG. 2. Typical $I-V$ curve measured between the Ag-coated AFM probe and the Ag film-counter electrode on $RbAg_4I_5$. The potential of Ag counter electrode versus AFM probe was swept from +100 to −100 mV at the rate of −100 mV/s. System measurement limits are ±10 nA. Exponential behavior implies that this deposition process is electrochemical reaction limited rather than diffusion limited in the bias range shown. A fit to the Butler–Volmer equation (dashed line) shows good agreement.

As discussed previously, the plot in Fig. 2 is a typical $I-V$ curve of the Ag-tip/$RbAg_4I_5$/Ag-film system acquired using the experimental setup shown in Fig. 1. ($RbAg_4I_5$ sample thickness: 0.52 mm, Ag counter electrode film area: ~0.5 cm^2). The $I-V$ curve data points in Fig. 2 can be fit to the Butler–Volmer equation [Eq. (1)], as shown by the dotted line,

$$i = i_0\left[\frac{C_{Ag^+}}{C^*_{Ag^+}}\exp\left(-\alpha\frac{F}{RT}\eta\right) - \frac{C_{Ag}}{C^*_{Ag}}\exp\left((1-\alpha)\frac{F}{RT}\eta\right)\right], \tag{1}$$

The close agreement between the Butler–Volmer equation and experimental data indicates that the deposition rate in ~±50 mV range is limited by electrochemical reaction kinetics rather than diffusion process inside the ion conductor. From the fit, we extract kinetic constants indicative of a fast electrochemical reaction (j_0=0.973 A/cm^2, α=0.396, $C_{Ag^+}/C^*_{Ag^+}$=0.637). In the future, understanding the kinetic and diffusion related constraints on the reaction for a given set of experimental conditions (e.g., bias amplitude, pulse

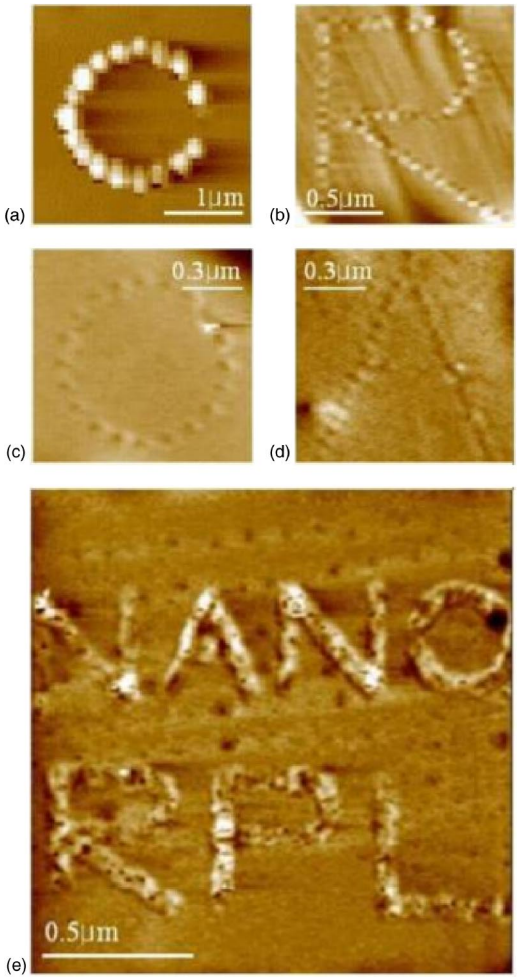

FIG. 3. AFM contact-mode deflection images of electrochemically induced Ag nano-features on $RbAg_4I_5$. (a) 50 nm high positive features generated by 200 mV, 5 ms pulses for each dot. (b) 2 nm high positive features generated by 400 mV, 1 ms pulses for each dot. (c) 6 Å deep negative features generated by 200 mV, 1 ms pulses for each dot. (d) 6 Å deep negative features generated by 200 mV, 1 ms pulses for each dot. (e) Positive features generated by 200 mV pulses. (Dot spacing =17 nm, pulse duration =0.25 ms for upper letters. Dot spacing =22 nm, pulse duration =0.30 ms for lower letters.)

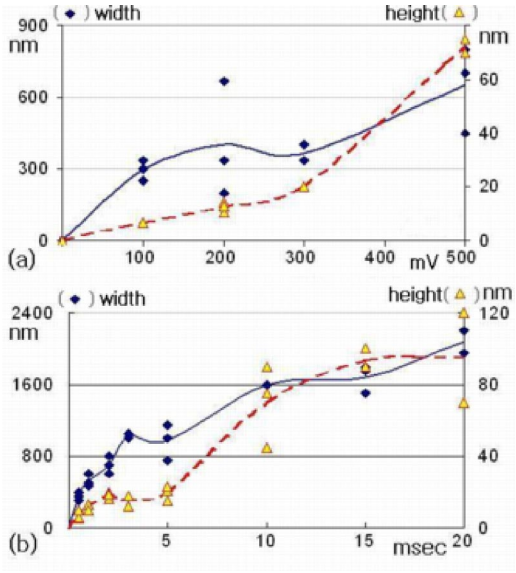

FIG. 4. Plot of feature size (◆) and height (△) as a function of bias voltage. The duration of pulse is 20 ms. (b) Plot of feature size (◆) and height (△) as a function of bias duration. The amplitude of pulse is 2 V. Solid lines are fit curves for feature size and dotted lines are for feature height.

duration, etc.) should give us more precise predictive control over the nanopatterning process.

Figure 3 shows positive [(a), (b), and (e)] and negative [(c) and (d)] patterns made from sequences of dots generated by applying bias voltage pulses of 200–400 mV for 0.25–5 ms. The thickness of $RbAg_4I_5$ was 0.5 mm and the Ag film counter electrode area was around 0.1 cm^2. (See Fig. 1). Formation of negative features, such as the ones shown in Figs. 3(c) and 3(d) is due to mechanical knock-off of the deposited clusters by the AFM probe during topography scan. Negative features larger than a few hundred nanometers are rarely observed because the adhesion between the deposited Ag cluster and the substrate sample becomes stronger as the feature size grows larger.

As can be seen from Fig. 4(a), the size of patterned feature tends to more or less linearly grow as the bias voltage increases. The feature height, on the other hand, follows rather an exponential behavior versus bias voltage. From these two plots, it can be deduced that high pulsing voltages tend to give high aspect ratio features.

In summary, this AFM-aided nanopatterning technique represents an alternative method in nanolithography by directing electrochemical reactions on a solid-state ionic conductor to electrically induce patterning. Sub-100 nm features have been routinely patterned by applying pulses on the order of several hundred millivolts in the millisecond time frame. Several examples of positively and negatively patterned features were presented (Fig. 3). It has been observed that negative features are created by a mechanical knock-off of previously deposited Ag nano-clusters by the AFM probe during the subsequent topology scan. Optimal resolution and consistency requires smooth and clean sample surfaces and sharp conductive AFM tips.

Materials that can be patterned through the present process are not restricted to silver. A variety of other solid-state ion conductors for Li^+, Na^+, K^+, Cu^+, Pb^{2+}, and Ca^{2+} can be employed for patterning metal structures. Due to the swiftness of this process in generating patterns and the size of the resulting features, we conjecture this process to be suitable for erasable high-density data storage applications.

This work was financially supported by the Office of Naval Research (ONR) and the center for Scalable and Integrated Nano-Manufacturing (SINAM) of University of California in Los Angeles.

[1]G. Y. Liu, S. Xu, and Y. L. Qian, Acc. Chem. Res. **33**, 457 (2000).
[2]S. Xu and G. Y. Liu, Langmuir **13**, 127 (l997).
[3]S. Xu, S. Miller, P. E. Laibinis, and G. Y. Liu, Langmuir **15**, 7244 (1999).
[4]H. J. Mamin and D. Rugar, Appl. Phys. Lett. **61**, 1003 (1992).
[5]H. J. Mamin, Appl. Phys. Lett. **69**, 433 (1996).
[6]E. A. Dobisz and C. R. K. Marrian, Appl. Phys. Lett. **58**, 2526 (l991).
[7]C. R. K. Marrian, E. A. Dobisz, and J. A. Dagata, J. Vac. Sci. Technol. B **10**, 2877 (1992).
[8]A. Majumdar, P. I. Oden, J. P. Carrejo, L. A. Nagahara, J. J. Graham, and J. Alexander, Appl. Phys. Lett. **61**, 2293 (1992).
[9]L. L. Sohn and R. L. Willett, Appl. Phys. Lett. **67**, 1552 (1995).
[10]D. M. Kolb, R. Ulmann, and T. Will, Science **275**, 1097 (1997).
[11]D. Hofmann, W. Schindler, and J. Kirschner, Appl. Phys. Lett. **73**, 3279 (1998).
[12]R. J. Randler, D. M. Kolb, B. M. Ocko, and I. K. Robinson, Surf. Sci. **447**, 187 (2000).
[13]R. Schuster, V. Kirchner, X. H. Xia, A. M. Bittner, and G. Ertl, Phys. Rev. Lett. **80**, 5599 (l998).
[14]J. A. Dagata, J. Schneir, H. H. Harary, C. J. Evans, M. T. Postek, and J. Bennett, Phys. Rev. Lett. **56**, 2001 (1990).
[15]H. C. Day and D. R. Allee, Appl. Phys. Lett. **62**, 2691 (1993).
[16]E. S. Snow and P. M. Campbell, Appl. Phys. Lett. **64**, 1932 (l994).
[17]L. Santinacci, T. Djenizian, and P. Schmuki, Appl. Phys. Lett. **79**, 1882 (2001).
[18]R. D. Piner, J. Zhu, F. Xu, S. H. Hong, and C. A. Mirkin, Science **283**, 661 (l999).
[19]S. H. Hong and C. A. Mirkin, Science **288**, 1808 (2000).
[20]Y. Li, B. W. Maynor, and J. Liu, J. Am. Chem. Soc. **123**, 2105 (2001).
[21]G. Agarwal, R. R. Naik, and M. O. Stone, J. Am. Chem. Soc. **125**, 7408 (2003).
[22]S. Geller, *Solid Electrolytes*, edited by S. Geller (Springer, Berlin, 1977).
[23]H. Kennedy, F. Chen, and J. Hunter, J. Electrochem. Soc. **120**, 454 (1973).
[24]R. O'Hayre, M. Lee, and F. B. Prinz, J. Appl. Phys. **95**, 8382 (2004).